

Development of vertical electropolishing process applied on 1300 and 704 MHz superconducting niobium resonators

F. Eozénu,^{*} Y. Boudigou, P. Carbonnier, J-P. Charrier, Y. Gasser, L. Maurice,
F. Peauger, D. Roudier, and C. Servouin
CEA, Irfu, SACM, Centre de Saclay, F-91191 Gif-Sur-Yvette, France

K. Muller

Phelma–Grenoble INP–38016 Grenoble Cedex 1, France

(Received 7 March 2014; published 21 August 2014)

An advanced setup for vertical electropolishing of superconducting radio-frequency niobium elliptical cavities has been installed at CEA Saclay. Cavities are vertically electropolished with circulating standard HF-HF-H₂SO₄ electrolytes. Parameters such as voltage, cathode shape, acid flow, and temperature have been investigated. A low voltage (between 6 and 10 V depending on the cavity geometry), a high acid flow (25 L/min), and a low acid temperature (20°C) are considered as promising parameters. Such a recipe has been tested on single-cell and nine-cell International Linear Collider (ILC) as well as 704 MHz five-cell Super Proton Linac (SPL) cavities. Single-cell cavities showed similar performances at 1.6 K being either vertically or horizontally electropolished. The applied baking process provides similar benefit. An asymmetric removal is observed with faster removal in the upper half-cells. Multicell cavities (nine-cell ILC and five-cell SPL cavities) exhibit a standard Q_0 value at low and medium accelerating fields though limited by power losses due to field emitted electrons.

DOI: [10.1103/PhysRevSTAB.17.083501](https://doi.org/10.1103/PhysRevSTAB.17.083501)

PACS numbers: 74.70.Ad, 81.65.Ps, 82.47.Wx, 82.45.Qr

I. INTRODUCTION

Electropolishing in hydrofluoric-sulfuric acid mixtures has become the reference process to reach high performance on niobium cavities [1] in accordance with the requirements of recent projects such as Continuous Electron Beam Accelerator Facility upgrade [2], X-ray Free Electron Laser linac [3], and future International Linear Collider (ILC). According to the standard process, the cavity is electropolished in a horizontal position, while rotating and half filled with circulating acid. Vertical electropolishing (VEP) is studied in some laboratories as an alternative [4–10]. The aim is to develop an easier process compared to horizontal electropolishing (HEP), while providing similar performance, in order to achieve a cost-effective production of cavities for upcoming large-scale projects in the near future. As an example, the construction of the ILC requires the treatment of 16 000 cavities for the 500 GeV baseline configuration.

High gradients have already been achieved by VEP with stirred static acid [11,12] but only for final thin removal; for deeper removal a Q slope is observed [12]. We anticipate that a circulation of the acid mixture and a better acid

renewal should provide improved electropolishing conditions. An automated VEP device with a circulating acid system has been developed at CEA Saclay (see Fig. 1). The cavity is filled from the bottom and the acid runs back to the tank by gravity from the top of the setup. The technical



FIG. 1. Five-cell SPL cavity during VEP treatment.

^{*}fabien.eozenou@cea.fr

Published by the American Physical Society under the terms of the Creative Commons Attribution 3.0 License. Further distribution of this work must maintain attribution to the author(s) and the published article's title, journal citation, and DOI.

characteristics of this setup are detailed elsewhere [5]. It has been designed for the treatment of elliptical cavities, from 1.3 GHz single-cell to 704 MHz five-cell cavities designed for the Superconductive Proton Linac (SPL) [13].

As a first step, single-cell Tesla-shaped cavities have been used to commission the setup and optimize the parameters. Then, multicell (SPL five-cell and ILC nine-cell) cavities have been electropolished. Results will be presented for these 1300 and 704 MHz superconducting niobium resonators.

II. PARAMETERS STUDY ON SINGLE-CELL 1300 MHz TESLA-SHAPED CAVITY

Vertical electropolishing at a voltage of 20 V has already been investigated on single-cell cavities [5], and a gradient of 30 MV/m has been achieved. In a second step, single-cell cavities have been electropolished with parameters derived from standard horizontal EP: (i) moderate acid flow (8 L/min); (ii) voltage above 12 V; (iii) temperature around 30°C. The electrolyte is a mixture of HF(40w%) – H₂SO₄(96w%) in volume proportions of 1 to 9. The cathode chosen for these experiments consists in a rod shape with a small protuberance (20 mm in length and 50 mm in diameter). This cathode is used in [5].

We applied those parameters to the single-cell Tesla-shaped cavity “1AC3.” The inner surface inspection was performed and revealed that these parameters are not compatible with proper electropolishing conditions. In fact, the surface is deteriorated after 70 μm removal on average: a ring of pits is observed between the equator and iris of the upper half-cell (see Fig. 2). The local removal rate is above 1 $\mu\text{m}/\text{min}$. It is too high for desirable electropolishing conditions, if considering the appropriate rate is 0.6 $\mu\text{m}/\text{min}$ for HEP.

The location of pits coincides with a singularity of the fluid distribution modeled at low fluid velocity which will be mentioned later in Fig. 7. Furthermore, the presence of hydrogen bubbles insufficiently evacuated by the acid flow might also amplify this phenomenon. Thickness measurements using an ultrasonic gauge were carried out, at six locations of the cell [Fig. 2(c)]. The gauge was calibrated using a niobium plate. At one location, the spans can be explained by the nonflatness of the cavity and therefore, an uncertainty is introduced while positioning reproducibly the sensor. The removal on the upper or lower half-cell is well illustrated in Table I.

As a consequence, we decided to increase the acid flow up to 25 L/min in the following VEP sequences so as to improve the fluid distribution (symmetry in the cell) and the hydrogen evacuation out of the cavity. This would allow both efficient acid renewal and temperature control (electrolyte at 20°C) inside the cavity. Nitrogen is also blown in the acid tank and at the top end group of the cavity in order to prevent any explosion risk and to favor the

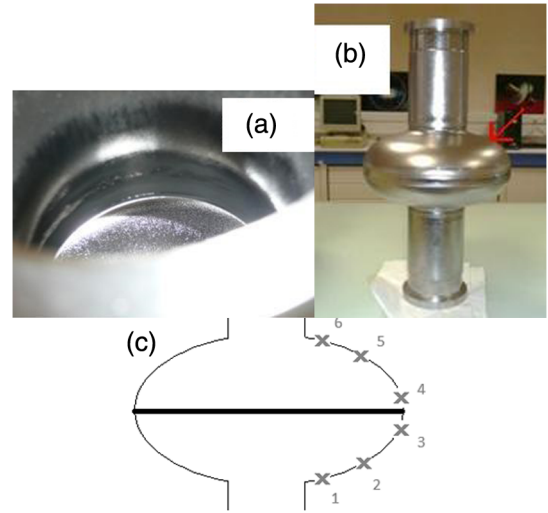


FIG. 2. (a) Inspection of the inner surface of “1AC3” cavity after VEP at 12 V – 30°C. A ring of pits is observed at the location indicated by a red arrow on (b). For further study of material removal, single-cell cavities were carved at six locations according to (c).

removal of the gas generated during the process. Previous EP investigations showed that a reduced electropolishing voltage (down to 5 V) has no influence on cavity performance (a process called “low-voltage electropolishing”) [14]. We decided to apply low-voltage VEP with the following expectations: (i) a decreased joule heating and decreased temperature gradient in the cavity and (ii) reduced parasitic electrochemical reactions as sulfur forms [14–17].

A higher acid flow rate is thus expected to provide improved electropolishing conditions. The highlighted set of parameters was applied on the single-cell Tesla-shaped cavity “1DE1,” which was previously horizontally electropolished, in order to compare the two techniques. After 70 μm additional VEP, the achieved surface is very shiny. The average removal rate is 0.2 $\mu\text{m}/\text{min}$. No pitting is observed though shallow stripes are observed at the equator area in the upper half-cell. The new set of parameters seems promising and the performance of the cavity at 1.7 K will be evaluated.

TABLE I. Measured material removal at 6 locations in the cavity at 6 V and 8 L/min acid flow rate. Fluid circulates from bottom.

	Average removal (μm)	100
	Removal at location #1	80–90
	#2	50
	#3	60–70
	#4	80–100
	#5	160–180
	#6	210–240

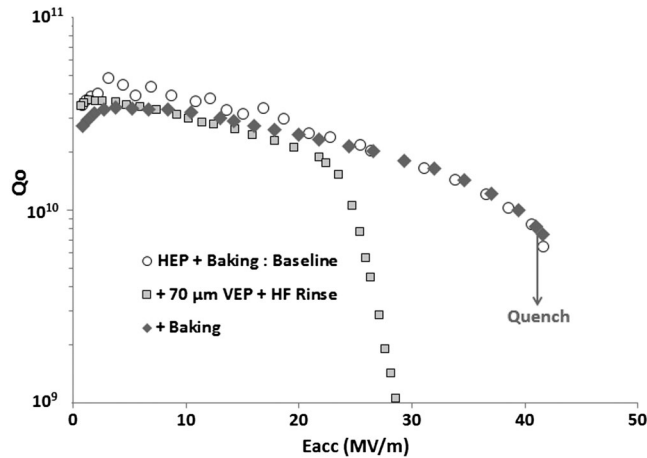


FIG. 3. Radio-frequency results of the “1DE1” cavity at 1.6–1.7 K before/after VEP at 6 V. The baking process has been performed at 137°C during 60 h.

III. RESULTS ON 1300 MHZ CAVITY WITH OPTIMIZED PARAMETERS

A. Results on single-cell cavities

The performance of the 1DE1 as received (after HEP) was very high ($E_{acc} > 42$ MV/m, high Q_0). It was tested at 1.6–1.7 K after the additional 70 μm low-voltage VEP sequence. The cavity was rinsed with diluted hydrofluoric acid before the presented test in order to remove possible contamination resulting from a leak. The rf tests in vertical cryostat were performed before and after baking at 137°C during 60 h. $Q_0 = f(E_{acc})$ plots are shown in Fig. 3. The following results can be observed: (i) the baking effect is similar compared to HEP: the Q slope at high field is removed and the performance was limited by quench at $E_{acc} > 40$ MV/m; (ii) the $Q_0 = f(E_{acc})$ plots after HEP and after VEP agree very well. Low-voltage VEP offers similar performance compared to HEP.

In a second step, we intend to achieve similar performance with a cavity that has been exclusively electropolished. Additional tests were carried out on the 1AC3 cavity. The 1AC3 cavity, as described in Fig. 2, was again electropolished according to two VEP sequences with “optimized” parameters and baked under vacuum (110°C \times 60 h). After each sequence, it was tested at 1.6 K (see results in Fig. 4). The gradient reached 35 MV/m gradient, in spite of the pitted surface. The performances were limited by a quench located at the pitted area with both thermal sensors and oscillating superleak transducers. Moreover the gradient was improved after additional VEP sequence at low voltage, though the Q_0 value was degraded.

The presented preliminary results on Tesla-shaped single-cell cavities show that the described VEP treatment offers potentials similar to the standard HEP. A Q slope is observed after VEP, which is removed by baking. VEP

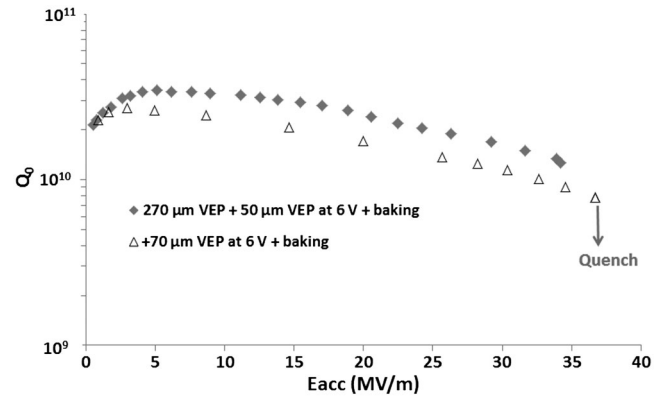


FIG. 4. Radio-frequency results of the “1AC3” cavity at 1.6–1.7 K after VEP sequences at 6 V and baking.

allows one to reach gradients similar to those obtained with standard horizontal EP treatment. The decrease in Q_0 after the last VEP treatment on the 1AC3 cavity is not understood yet.

B. Results on a ILC nine-cell cavity

The same set of parameters (6 V – 20 L/min – $T < 20^\circ\text{C}$) was applied on a nine-cell cavity: 50 μm on average were removed from the “TB9R1025” ILC cavity from Fermi Accelerator National Laboratory (FERMILAB), previously horizontally electropolished. A large cathode diameter (50 mm) was used for nine-cell VEP experiments in [5] in order to decrease the anodic current density. The diameter was reduced down to 40 mm for this experiment in order to avoid contact with HOM antennas during insertion. Unfortunately, the performance was limited by field emission, with onset at 15 MV/m. The Q_0 value at low and medium fields is satisfactory (see Fig. 5).

Additional VEP sequences and cleanroom assembly are planned for improvement.

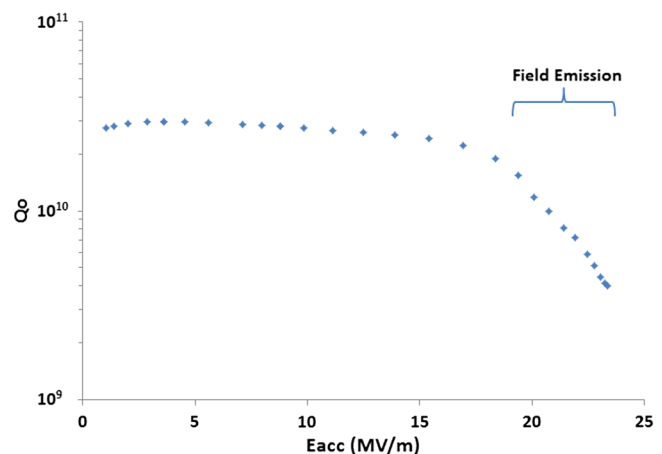


FIG. 5. Radio-frequency results of the “TB9R1025” ILC cavity at 1.7–1.8 K after HEP + 50 μm VEP at 6 V.

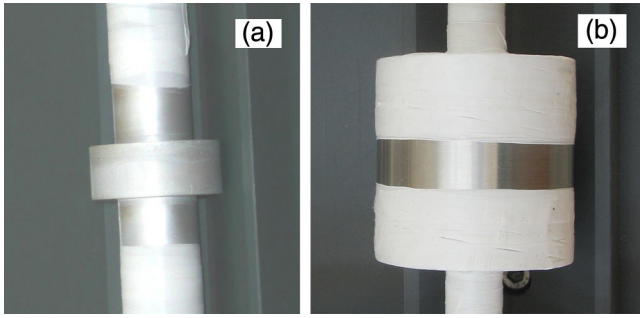


FIG. 6. (a) Cathode used in previous VEP experiments (shape #1) and (b) optimized shape (shape #2).

IV. CATHODE DESIGN AND ASYMMETRY OF THE PROCESS

A. Alternative cathode shapes

The possible benefits of alternative cathode shapes have been widely investigated [7–9,18–22]. The effectiveness of an optimized electrical field in the case of the buffered electrochemical polishing treatment (electrolyte involving additional acid lactic) [23] has been demonstrated [7]. Alternative shapes have been proposed in order to improve the homogeneity of the process. We have decided to focus on cathode shapes compatible with an easy insertion in the cavity (narrower than the diameter of the beam pipe). The work done in [5] was pursued with a more exhaustive study [22]: a design of experiment method was carried out using COMSOL software in order to obtain both uniform electric field and fluid distribution inside the cell. Dominant parameters that have been put forward are (i) the shape of the cathode (ellipsoid or cylindrical) and (ii) the length and diameter of the protuberance. The optimized cathode is shown in Fig. 6(b) (shape #2).

Its shape is a cylinder (70 mm in diameter and 70 mm in length). Figure 7 shows the fluid distribution inside the cell at low flow rate (<5 L/min): the vortex created with shape #1 should be suppressed with the cylindrical shape.

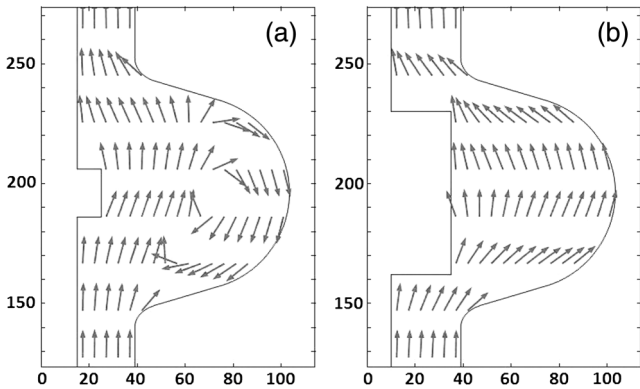


FIG. 7. Direction of the flow modeled with COMSOL for VEP with shape #1 (a) and #2 (b) for low acid flow rate.

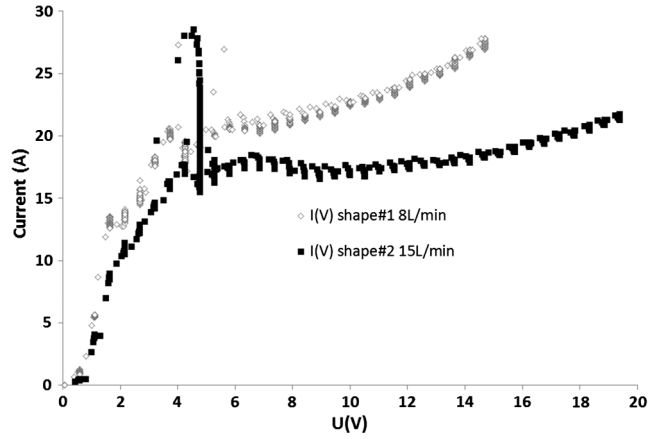


FIG. 8. $I(V)$ curves plotted on single-cell cavity with cathode shape #1 & #2.

The electropolishing process is limited by the diffusion of the fluorine ions [14,24] in the presence of a surface film [25]. The signature of this diffusion is the plateau observed on $I(V)$ curves. Such curves were plotted during VEP of a Tesla shaped single-cell cavity using both cathode shapes. Shape #2 associated with a higher flow rate is efficient to obtain a wider diffusion plateau, clearly visible in Fig. 8.

B. Asymmetry of the process

The effect of the cathode shape on the symmetry of the material removal in the cell has been further investigated. For the optimized set of parameters (25 L/min, 6 V, $T = 20^\circ\text{C}$), thickness measurements have been carried out after VEP sequences in additional configurations: (i) shape #2 : insulated; (ii) shape #2 : naked; and (iii) 30 mm diameter rod cathode : naked. The results are given in Table II.

We clearly notice the effect of the shape/insulation in configuration A, on the lower half-cell: the removal in locations #1, #2, and #3 is fairly uniform. However, this gain is balanced by a strong vertical asymmetry with the deeper removal in the upper half-cell. The removal at

TABLE II. Measured material removal at six locations in single-cell Tesla-shaped cavities (1AC1, 1AC2, and 1AC3) for different cathode configurations.

Configuration	A	B	C
Cathode	Shape #2	Shape #2	30 mm Rod
Insulated	Yes	No	No
Average removal (μm)	120	60	90
Removal at #1	50	40–50	30–40
#2	40	30	30–40
#3	50	10–20	60–70
#4	100	50	80
#5	200	110	100
#6	290	150–180	160–170

location #6 is roughly 6 times deeper than the removal at location #1. In configuration C, the removal is less uniform in the lower half-cell, but the vertical asymmetry is decreased.

Similarly to [7], we have to consider in this study the viscous layer that is generated at the niobium surface during VEP. The benefits of improved electric field and fluid distribution are lowered by the macroscopic movement of the viscous surface film, highlighted on flat samples in [26–27]. The two half-cells should be distinguished during VEP: (i) in the upper half-cell, the layer runs or slides down the cavity due to the gravity. In some areas, the surface might be “viscous layer depleted.” (ii) In the lower half-cell, the surface is smooth due to the thicker layer but the removal is thin due to its high electric resistance.

Furthermore, in the upper part of the cell, the electric current might be more sensitive to increased hydrodynamic flow (acid as well as generated hydrogen). Because of the bended flow [highlighted in Fig. 7(b)], the shape of the cathode would then guide hydrogen bubbles to the surface of the cavity. It might be responsible for the stripes observed and for increased convection. The difference between the configurations of rod/shaped cathodes might be described in the following schematic (Fig. 9).

Considering these results, we conclude that a rod cathode is more appropriate for the vertical EP configuration, because of the better hydrogen removal and resulting decreased asymmetry between the upper and the lower half-cells. Alternatives are investigated in different laboratories, for example, the use of a patented rotating retractable cathode at Marui Galvanizing Company in Japan [8]. The use of a mock-up in plastic proved the resulting improvement of the mixing of the fluid, especially at low flow rate.

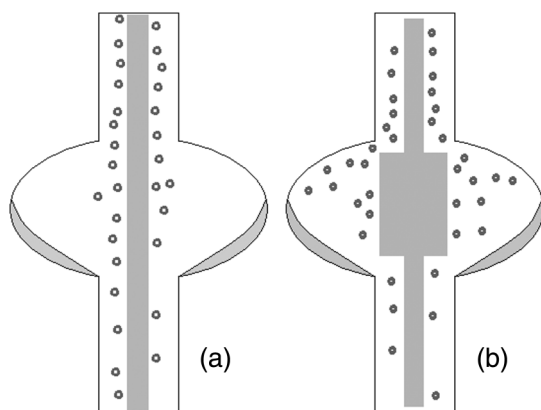


FIG. 9. Schematics of the assumed hydrogen/viscous layer distribution during VEP for two cathode shapes. The drawings are not in the correct scale. With a rod cathode (a), hydrogen runs along it, but in the case of the cathode #2, bubbles are likely to reach the surface in a viscous layer-depleted area, and this configuration generates a faster removal.

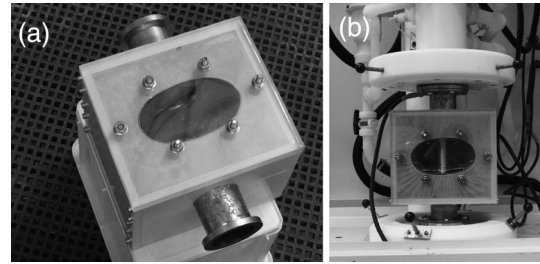


FIG. 10. (a) Mock-up for the viewing of the inside of a single-cell cavity during VEP and (b) setup ready for VEP.

For better understanding of the fluid distribution during treatment using a fixed cathode, a mock-up was designed at CEA Saclay in order to observe the inside of a cavity during the VEP process. It consists of a cut single-cell cavity embedded in a resin box, and closed with a transparent window, as shown in the pictures in Fig. 10.

This modified cavity was electropolished with circulating acid using a rod cathode for several minutes. Once the cavity is filled, the voltage is applied between the cavity and the cathode. It is observed that hydrogen bubbles are generated in curls and run along the cathode, driven by the acid flow. This observation agrees with the result of the flow model [5]. No visible bubbles are stuck at the cavity surface. We have observed the effect of the pulse of the membrane pump: the pressure pulses induce the destruction of the H_2 curls into constellations of smaller bubbles that are more likely to diffuse in the electrolyte.

Besides, a distinct aspect has to be considered: the filling rate of the cavity. At a high filling rate (30 L/min), air bubbles are observed (several mm in diameter) that are stuck at the upper side of the cell. These bubbles are immobile and are not evacuated by the acid flow. Filling of the cavity at a lower rate (<10 L/min) prevents the formation of these air bubbles.

V. EXPERIMENTS ON SPL 704 MHZ FIVE-CELL CAVITY

The VEP technique has been applied to a 704 MHz five-cell SPL cavity, with $\beta = 1$ (dimensions in mm are given in Fig. 11) in order to match challenging gradients (25 MV/m) targeted in the EuCARD project [13].

A. Profile of material removal

The efficient evacuation of hydrogen is considered a major challenge for vertical EP. It is confirmed in this demanding configuration, due to the large volume (~ 90 L) and the large niobium surface (1.76 m²) of the cavity. VEP sequences were carried out at 10 V instead of 6 V for a 1300 MHz cavity, because satisfactory polishing conditions have been observed on a single-cell 704 MHz cavity under this voltage [9,28]. We used a rod cathode (70 mm in diameter) in aluminum. The acid flow was high (between

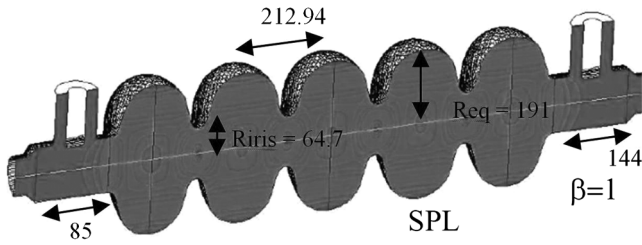


FIG. 11. 704 MHz SPL cavity and characteristic dimensions.

20 and 25 L/min). It corresponds to the upper admissible flow for the setup, which allows one to decrease the temperature rise in the cavity and facilitate hydrogen removal. The temperature rise in the cavity was less than 5°C for an inlet temperature of around 10°C. The niobium removal in the cavity was measured after several sequences (measurement by ultrasonic gauge). The cavity was systematically turned over between two VEP treatments. After the first main sequence (60 μm removal), a very strong attack resulting in a rough surface at the upper position near the iris in cell #5 was observed. Some pits were also observed after this sequence. The measured removal profile is shown in Fig. 12 (black squares).

The monitoring of hydrogen inside the treatment cabinet was considered afterwards and unexpected peaks have been observed. Such a release of hydrogen should not happen thanks to the nitrogen venting in the upper part of the acid tank and at the upper end group of the cavity by the extraction system. After inspection of the setup, we found some acid condensation in the gaseous exhaust pipe preventing gases from being extracted. The incriminated pipe was drained.

A VEP sequence was carried out with the same cavity orientation, and the material removal profile in this configuration is shown in the second curve (white triangles) of Fig. 12. An asymmetry in each cell (similar to the 1300 MHz case), with an additional effect of the position of the cell, are observed. The removal in a cell increases with its vertical position. The removal is more pronounced in the two upper cells.

After the four main VEP sequences, the removal of the cavity evaluated by weighing was 200 μm in average and the distribution of removal is shown in Fig. 13.

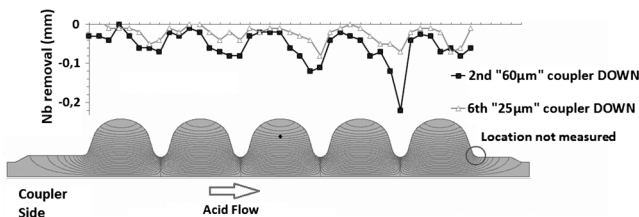


FIG. 12. Niobium removal during two different VEP sequences with the same cavity orientation. The removal in the upper cells is dramatic if hydrogen is not properly evacuated (black curve).

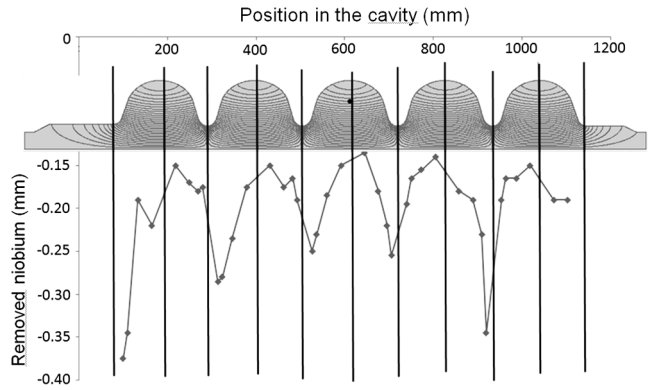


FIG. 13. Distribution of niobium removal after the four main VEP sequences, which corresponds to the removal of 200 μm in average.

We observe that turning of the cavity allows one to obtain a symmetric removal around the center of the cavity. The highest local rate in cell #5 results from deteriorated conditions during the VEP sequence with no hydrogen extraction previously described (already highlighted in Fig. 12.). We might also notice that the removal rate at the equators is half the rate at the irises. This ratio is similar to the horizontal EP case with 1300 MHz resonators [29], even though the configuration is less favorable (lower electric field at equators due to the larger diameter of the cavity). The nonuniform electric field distribution inside the cell during EP is generally put forward as the explanation. The movements of the resistive surface film due to the gravity during the process, accumulating at the equator, should rather be considered as the main component of the removal rate distribution in the HEP configuration.

B. Surface morphology

The internal surface of the cavity was investigated after substantial VEP treatments. The surface morphology varies along the cavity as shown in Fig. 14. Equators, where the highest rf magnetic field is located, are smoothed, as well as irises and beam pipes. In the areas located between each iris and equator, the surface appears to be rougher. Grain boundaries are more pronounced and features such as stripes are observed.

C. Field flatness

Field flatness has been measured after each VEP sequence. The first uncontrolled sequence resulted in a shift in the field profile (see the curve after 70 μm removal in Fig. 15). Once the problem was solved, no shift was observed.

D. 100 K effect

The vertically electropolished 704 MHz SPL cavity was tested in a vertical cryostat. On the accelerating mode

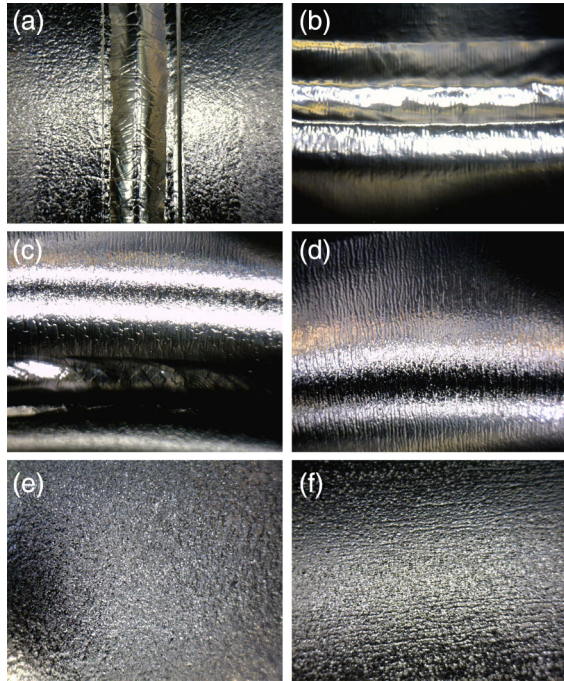


FIG. 14. Typical surface morphologies after substantial VEP ($>100 \mu\text{m}$) at different locations of the cavity. The weldings at (a) equators and (b) irises are smooth. Stripes caused by bubbles are observed at the proximity of irises (c) and (d). In the areas between equators and irises (e), the surface is rougher. Some pitting occurred during the uncontrolled VEP sequence (f). The width of the each view is approximately 20 mm.

(π -mode) the measured Q_0 at low accelerating gradient (below 1 MV/m) was 2×10^9 at 1.5 K, which is approximately 10 times lower than expected. When increasing the gradient up to 6 MV/m the Q_0 decreased quickly down to 5×10^8 , with a dissipated rf power of 150 W in the cavity.

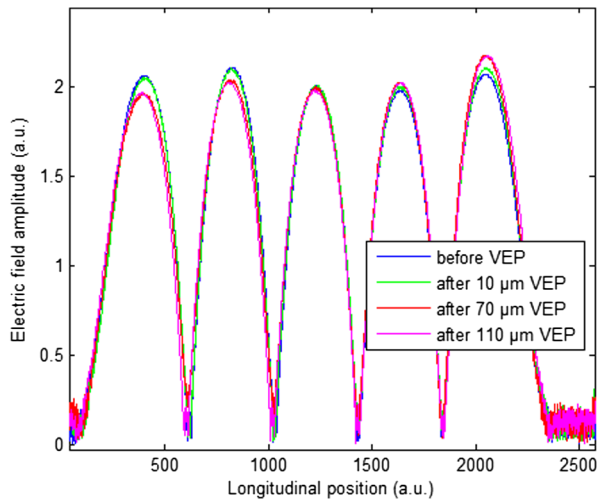


FIG. 15. Field flatness evolution after each VEP sequence. After the second sequence (uncontrolled process), a shift is observed. No deterioration is noticed once the hydrogen problem has been solved.

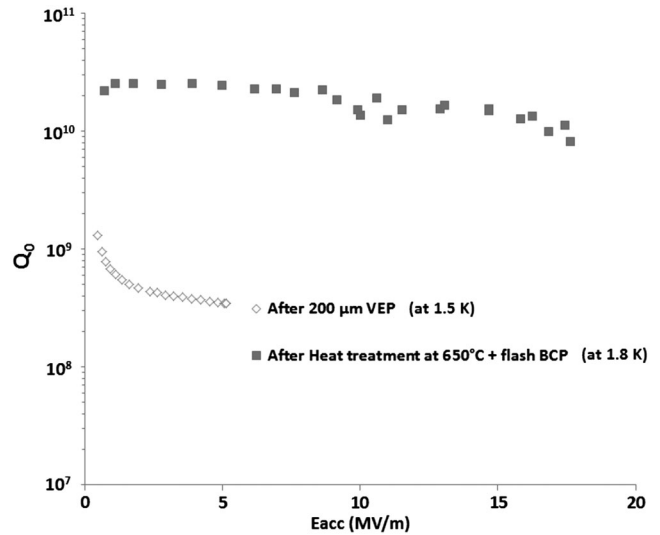


FIG. 16. Tests of the SPL cavity in vertical cryostat before and after heat treatment. The heat treatment at 650°C efficiently cured the hydrogen contamination. The test was stopped at 18 MV/m because of the too high radiation level (field emission onset at 10 MV/m). An additional test is planned at higher gradients.

The tests have been stopped at this rf power level. This fast Q slope is observed when a “ Q disease (100 K effect)” is produced in the cavity [30]. It corresponds to the formation of niobium hydride at the surface of the cavity. The phenomena is enhanced when the cool down of the cavity is not fast enough (typically staying at a temperature between 150 K and 50 K for longer than 1 h). In order to remove the incriminated hydrogen, a heat treatment of the cavity under vacuum at 650°C for 24 h was carried out at CERN.

The final surface treatment before the additional test of the cavity was a light buffered chemical polishing (less than $10 \mu\text{m}$) with a standard mixture of hydrofluoric, nitric, and phosphoric acids (ratio 1:1:2.4) to remove possible contamination from the oven.

The quality factor was significantly improved after heat treatment with a value over 2×10^{10} at 1.8 K. (See Fig. 16.) Field emission occurred at high gradient and the test was stopped at 18 MV/m because of the high radiation level measured in the testing hall. Additional tests are planned at higher gradients after the modification of the test area.

VI. OUTLOOK AND CONCLUSION

Low-voltage (6 V), high acid flow (25 L/min), and low acid temperature (20°C) are considered as promising parameters for VEP of 1300 MHz cavities. Such a recipe was tested on single-cell and nine-cell ILC cavities. After $70 \mu\text{m}$ VEP on a single-cell cavity, it showed similar performance at 1.6 K compared to previous horizontal EP (Eacc > 41 MV/m) limited by quench. VEP with

circulating acid is promising at least for final treatment after bulk EP/tumbling, etc. Another cavity reaches 36 MV/m after heavy removal by VEP in spite of a pitted initial surface. The baking effect after VEP is similar to HEP. Nice surface finishing as well as a standard Q_0 value are obtained at low/medium fields on a nine-cell 1300 MHz cavity. Unfortunately, the performance of the tested cavity was limited by field emission. An asymmetric removal is observed with faster removal in the upper half-cells.

The configuration is more challenging in the case of 704 MHz cavities because of the larger volume of hydrogen to be generated. A deficient evacuation of this hydrogen is responsible for a faster attack in the upper cell, and pitting of the surface. A five-cell SPL cavity with $\beta = 1$ has been vertically electropolished with a rod cathode. Thanks to cavity turning between sequences, a symmetric material removal in the cavity is achieved. No significant modification of the field flatness is observed after each VEP sequence, once the hydrogen flow is evacuated properly. The cavity has been tested at 1.5 K and showed heavy Q disease (100 K effect). Heat treatment at 650°C allowed recovery of the expected Q_0 value. The gradient is presently limited to 18 MV/m because of the radiation level.

The VEP treatment of five-cell 704 MHz cavities for the European Spallation Source with $\beta = 0.86$ will also be investigated. These cavities differ from the SPL cavity with straight beam pipes (no taper), which should facilitate the fluid circulation. Besides, improvements of the existing machine are planned in order to improve gaseous evacuation during VEP treatments. They consist in enclosing the cathode with a meshed net in Teflon and in increasing the volume of the upper end group of the setup.

ACKNOWLEDGMENTS

We acknowledge the support of the European Community-Research Infrastructure Activity under the FP7 program (EuCARD, Contract No. 227579). This work has been carried out with the financial support of the “Conseil General de l’Essonne” in the frame of the ASTRE program. This work was possible thanks to Dr. C. Ginsburg from FERMILAB who provided the ILC cavity and Dr. D. Reschke from DESY for the loan of the 1DE1 Tesla single-cell cavity. We are also grateful to Dr. S. Calatroni and A. Mongelluzzo who made the heat treatment of the SPL cavity possible at CERN. We thank Dr. C. Madec for fruitful comments and proofreading of this work.

-
- [1] K. Saito *et al.*, in *Proceedings of the 8th Workshop on RF superconductivity (SRF 1997)*, AbanoTerme (Padova), Italy, 1997, edited by V. Palmieri (INFN, Padova, Italy, 1998), pp. 795–813.
- [2] A. Burrill *et al.*, in *Proceedings of the 2nd International Particle Accelerator Conference, IPAC-2011, San Sebastián, Spain* (EPS-AG, Spain, 2011), MOOCA01, pp. 26–28.

- [3] D. Reschke, in *Proceedings of the 15th International Workshop on RF Superconductivity (SRF 2011)*, Chicago, 2011, edited by M. Power, (JAcOW, 2012), MOIOA01, pp. 2–6.
- [4] R. L. Geng *et al.*, in *Proceedings of the 12th International Workshop on RF Superconductivity (SRF 2005)*, Cornell University, Ithaca, NY, 2005, edited by S. Bolomestnykh, M. Liepe, and H. Padamsee (LEPP, Cornell University, Ithaca, NY, 2007), THP04, pp. 459–463.
- [5] F. Éozéno, S. Chel, Y. Gasser, C. Servouin, B. Visentin, J-P. Charrier, and Z. Wang, *Phys. Rev. ST Accel. Beams* **15**, 083501 (2012).
- [6] S. Calatroni *et al.*, in *Proceedings of the 25th Linear Collider Conference (LINAC 2010)*, Tsukuba, Japan, 2010, edited by H. Sako (JAcOW, 2011), THP032, pp. 824–826.
- [7] S. Jin, A. T. Wu, X. Y. Lu, R. A. Rimmer, L. Lin, K. Zhao, J. Mammosser, and J. Gao, *Appl. Surf. Sci.* **280**, 93 (2013).
- [8] K. Nii *et al.*, in *Proceedings of the 16th International Workshop on RF Superconductivity (SRF 2013)*, Paris, France, 2013, edited by G. Martinet (IN2P3, Paris, 2014), TUP052, pp. 524–530.
- [9] L. M. A. Ferreira *et al.*, in [8], TUP047, pp. 512–514.
- [10] F. Furuta *et al.*, in [8], TUP049, pp. 518–520.
- [11] Z. A. Conway *et al.*, in *Proceedings of the 14th International Workshop on RF Superconductivity (SRF 2009)*, Berlin, Germany, 2009, edited by M. Abo-Bakr, B. Kuske, A. Liebezeit, S. Voronenko, and V. Schaa (SRF, Berlin, 2009), TUPPO004, pp. 176–179.
- [12] F. Furuta *et al.*, in *Proceedings of the 3rd International Particle Accelerator Conference, New Orleans, LA, 2012* (IEEE, Piscataway, NJ, 2012), TUPPR045, pp. 1918–1920.
- [13] J. Plouin *et al.*, in *Proceedings of the 15th International Workshop on RF Superconductivity (SRF 2011)*, Chicago, 2011, edited by M. Power (JAcOW, 2012) MOPO034, pp. 157–161.
- [14] F. Eozenou *et al.*, *Phys. Rev. STAccel. Beams* **13**, 083501 (2010).
- [15] K. Saito *et al.*, in *Proceedings of the 4th Workshop on RF Superconductivity (SRF 1989)*, Tsukuba, Japan, 1989, edited by Y. Kojima (National Laboratory for High-Energy Physics (KEK), Tsukuba, Japan, 1990), pp. 635–694.
- [16] A. Aspart, F. Eozéno, and C. Antoine, *Physica (Amsterdam)* **441C**, 249 (2006).
- [17] P. V. Tyagi, M. Nishiwaki, T. Saeki, M. Sawabe, H. Hayano, T. Noguchi, and S. Kato, *J. Vac. Sci. Technol. A* **28**, 634 (2010).
- [18] S. Calatroni *et al.*, in *Proceedings of the 11th workshop on RF superconductivity (SRF 2003)*, edited by D. Proch (DESY, Hamburg, 2004).
- [19] M. Bruchon *et al.*, in *Proceedings of the 13th International Workshop on RF Superconductivity (SRF 2007)*, Beijing, China, 2007, edited by J. Hao, S. Huang, and K. Zhao (Peking University, Beijing, China, 2009), TUP51, pp. 247–250.
- [20] N. Steinhilber-Kühl *et al.*, in [19], TUP33, pp. 204–206.
- [21] F. Eozenou *et al.*, in [8], TUP046, pp. 508–511.
- [22] K. Muller, CEA internal report, 2012.
- [23] A. T. Wu, J. Mammosser, L. Phillips, J. Delayen, C. Reece, A. Wilkerson, D. Smith, and R. Ike, *Appl. Surf. Sci.* **253**, 3041 (2007).

- [24] H. Tian and C. E. Reece, *Phys. Rev. ST Accel. Beams* **13**, 083502 (2010).
- [25] H. Tian, S. G. Corcoran, C. E. Reece, and Michael J. Kelley, *J. Electrochem. Soc.* **155**, D563 (2008).
- [26] F. Eozenou *et al.*, in CARE Report No. 06-10-SRF, 2006, CEA.
- [27] A. Chandra, M. Sumption, and G. S. Frankel, *J. Electrochem. Soc.* **159**, C485 (2012).
- [28] L. M. A. Ferreira (private communication).
- [29] TTC-Report 2008-05, http://flash.desy.de/sites/site_vuvfel/content/e403/e1644/e2271/e2272/infoboxContent2354/TTC-Report2008-05.pdf.
- [30] B. Bonin and R. W. Roth in *Proceedings of the 5th International Workshop on RF Superconductivity, Hamburg, German, 1991*, edited by D. Proch (DESY, Hamburg, 1992), p. 210.